Optical and magneto-optical properties of $Fe_{0.28}TaS_2$

1991 J. Phys.: Condens. Matter 3 6913

(http://iopscience.iop.org/0953-8984/3/35/021)

J. Phys.: Condens. Matter 3 (1991) 6913–6923. Printed in the UK

Optical and magneto-optical properties of $Fe_{0.28}TaS_2$

J H Wijngaard†, C Haas† and M A C Devillers‡

† Laboratory of Inorganic Chemistry, Materials Science Centre, University of Groningen, The Netherlands

‡ Research Institute for Materials, Faculty of Science, University of Nijmegen, The Netherlands

Received 30 March 1990, in final form 1 May 1991

Abstract. Ellipsometry and polar magneto-optical Kerr effect measurements were performed on $Fe_{0.28}TaS_2$ in the photon energy region 0.6–5 eV. The complex dielectric tensor was calculated from the measured data. Strong anisotropy was found in the diagonal elements of the dielectric tensor. Strong absorption bands at 1.6 and 3.8 eV for light polarized perpendicular to the *c*-axis were attributed to transitions between Ta 5d bands. In the off-diagonal element of the dielectric tensor five transitions with diamagnetic line shapes were observed. These transitions are between Fe 3d and Ta 5d states. The large magneto-optical contribution results from the large exchange splitting of the Fe 3d states combined with the large spin–orbit splitting of Ta 5d states.

1. Introduction

2H-TaS_2 is a layer compound consisting of hexagonal close-packed layers of Ta and S. In this way S–Ta–S sandwiches are formed in which Ta has a trigonal–prismatic coordination by S. In the sandwiches the chemical bonding is predominantly covalent, while the sandwiches are bonded to each other only by weak Van der Waals' interactions. This results in a compound with strongly anisotropic properties. The electrical resistivity, for example, is low (metallic) in the layers, while the resistivity perpendicular to the layers is much larger.

In the Van der Waals' gap between the sandwiches of 2H-TaS_2 a variety of atoms can be intercalated, including the 3d transition metals V, Cr, Mn, Fe, Co and Ni. The axis perpendicular to the layers (*c*-axis) is elongated as a result of the intercalation. The 3d atoms in the intercalated compound have a trigonally distorted octahedral coordination of S atoms. These 3d transition-metal intercalation compounds of TaS_2 have been studied extensively in the past (Parkin and Beal 1980, Parkin and Friend 1980a, b).

The magnetic moments in the 3d transition-metal intercalation compounds of TaS_2 order ferromagnetically or antiferromagnetically at temperatures below 30–130 K, depending on the 3d metal. All the 3d intercalation compounds of TaS_2 except the Fe compound have an easy axis of magnetization parallel to the layers. The exceptional behaviour of the Fe compound is caused by a non-zero angular momentum of the Fe^{2+} ions in the trigonally distorted octahedral coordination (Parkin and Friend 1980a). Because of the trigonal symmetry at the Fe site this momentum is directed perpendicular

0953-8984/91/356913 + 11 $03.50

to the layers. The spin angular momentum is coupled to the orbital angular momentum by spin–orbit interaction and is also directed perpendicular to the layers. This property makes the Fe intercalation compound interesting for a study of the polar magneto-optical Kerr effect. In the polar geometry of the magneto-optical Kerr effect the sample is magnetized perpendicular to the surface, while there is normal incidence of the light beam on the reflecting surface.

The electronic structure of TaS_2 intercalation compounds is usually discussed in terms of the rigid-band model (Parkin and Beal 1980). More recently the band structure of 2H-TaS_2 and $Fe_{1/3}TaS_2$ was calculated by Dijkstra *et al* (1989). These calculations show that important deviations from the rigid-band model occur. In both the host material 2H-TaS_2 and the intercalated compound there is a Ta $5d_{z^2}$ near the Fermi level that is split-off from the other unoccupied Ta 5d bands at higher energies. For the host material 2H-TaS_2 the Ta $5d_{z^2}$ band is half filled. During intercalation charge is transferred from the 3d atom to the Ta $5d_{z^2}$ band, resulting in a shift of the Fermi level to higher energies.

The Fe 3d bands are almost completely spin polarized. The Fe 3d bands for the majority spin electrons lie completely below the Fermi energy. In the density of states a crystal splitting of the Fe 3d bands arising from the trigonally distorted octahedral coordination of Fe is clearly observed. The Fe 3d bands for minority spin electrons lie almost completely above the Fermi level and also show the crystal-field splitting. There are a small number of spin-down electrons in this band. As a result the Fe atoms have an electronic configuration $(3d)^{5.4}$, and a local magnetic moment of $3.6\mu_B$ per Fe atom. There is also a small spin polarization of the Ta 5d and S 3p electrons, contributing a magnetic moment of $0.75\mu_B$ per Fe atom ($+0.10\mu_B$ on each Ta, $+0.075\mu_B$ on each S).

Measurements of the electrical transport properties of $Fe_{1/3}TaS_2$ were reported in the literature (Parkin and Friend 1980b, Dijkstra *et al* 1989). The observed positive Hall effect is in agreement with the expected conductivity by holes in the Ta $5d_{z^2}$ band. The observed value of the Hall coefficient also confirms the charge transfer from Fe to Ta in the intercalated compound.

In this paper we report on the optical and magneto-optical properties of $Fe_{0.28}TaS_2$. In section 2 some optical theory is briefly reviewed. In section 3 the experimental method is described and in section 4 the results of these experiments are presented. The results are discussed in section 5.

2. Theory

The propagation of light in a uniaxial (non-magnetic) crystal is described by a diagonal tensor with elements $\varepsilon_{xx} = \varepsilon_{yy}$ and ε_{zz}, where z is the principal optical axis of the crystal. All the tensor elements are complex: $\varepsilon_{ij} = \varepsilon'_{ij} - \varepsilon''_{ij}$.

For isotropic materials the three diagonal elements are all equal, and can be easily determined by ellipsometry (Azzam and Bashara 1987). For a uniaxial crystal the tensor elements can also be determined by ellipsometry, but a more complicated procedure is needed to derive the tensor elements from the measurements (Castelijns *et al* 1975). In this case measurements at two well chosen angles of incidence are needed to determine all the diagonal tensor elements.

Once the complex dielectric constants ε_{xx} and ε_{zz} are known, we can calculate the energy loss function

$$E_{\text{loss}} = \varepsilon''/(\varepsilon'^2 + \varepsilon''^2). \tag{1}$$

For a comparison with the band structure calculations the function $F = (\hbar\omega)^2\varepsilon''$ is an

important quantity. If one assumes constant matrix elements for the optical transitions, the function F is equal to the joint density of states (JDOS), which can be obtained from band structure calculations. The joint density of states is defined as

$$\text{JDOS} = A \sum_{\text{i,f}} \int \delta|E_{\text{f}}(\boldsymbol{k}) - E_{\text{i}}(\boldsymbol{k}) - \hbar\omega|\,\mathrm{d}v(\boldsymbol{k}) \tag{2}$$

where i and f denote initial (occupied) and final (unoccupied) electron states, $\boldsymbol{k}$ is the wavevector and A is a constant.

When considering the optical absorption of light by solids we can distinguish contributions from intraband and interband transitions (Hummel 1971). The dielectric constant can be written as

$$\varepsilon_{xx} = 1 - \frac{\omega_{\text{p}}^2}{\omega^2 - \mathrm{i}\omega\omega_{\text{s}}} + \sum_j \frac{Ne^2 f_j}{\varepsilon_0 m(\omega_j^2 - \omega^2 + \Gamma_j^2 + 2\mathrm{i}\omega\Gamma_j)}. \tag{3}$$

The intraband transitions (second term on right-hand side of equation (3)) are characterized by the plasma energy $\hbar\omega_{\text{p}}$ and the relaxation time for scattering τ, with $\omega_{\text{s}} = 1/\tau$. The contribution of the interband transitions can be described crudely by a sum of Lorentz-type terms (last term in equation (3)). The width at half maximum is $2\Gamma_j$, the average oscillator strength of all transitions of type j is f_j. The number of electrons involved is N, and ε_0 is the vacuum dielectric constant.

In a magnetic uniaxial crystal with the magnetization oriented parallel to the unique optical axis (z-axis), the non-diagonal elements ε_{xy} of the dielectric tensor determine the magneto-optical properties such as the magneto-optical Kerr effect (Freiser 1968). The value of ε_{xy} is usually small compared with the values of the diagonal elements of ε, and can be neglected in the ellipsometry determination of the optical constants.

The polar Kerr rotation, ϑ_{K}, and the ellipticity, ε_{K}, are related to the tensor elements by the relation

$$\vartheta_{\text{K}} + \mathrm{i}\varepsilon_{\text{K}} = \varepsilon_{xy}/[\varepsilon_{xx}^{1/2}(1 - \varepsilon_{xx})] \tag{4}$$

(conventions for the sign of the parameters for left- and right-hand circularly polarized light are those according to Azzam and Bashara (1987)). The contribution of interband transitions to the magneto-optical effects is given by (Kahn *et al* 1969):

$$\varepsilon_{xy} = \mathrm{i}\sum_k \frac{Ne^2(f_k^- - f_k^+)}{2m\varepsilon_0(\omega_k^2 - \omega^2 + \Gamma_k^2 + 2\mathrm{i}\omega\Gamma_k)}\left(\frac{\omega - \mathrm{i}\Gamma_k}{\omega_k}\right). \tag{5}$$

For a particular type of interband transition, k, the average transition energy is $\hbar\omega_k$, the parameter Γ_k is a measure of the range of energies over which the transitions of type k occur. The oscillator strength for left- and right-hand circularly polarized light are f_k^- and f_k^+, respectively. For one type of transition k, equation (5) leads to a so-called paramagnetic line shape for the real and imaginary parts of ε_{xy} (Kahn *et al* 1969, Wittekoek *et al* 1975). If two transitions with slightly different frequencies occur, one for left-hand and one for right-hand circularly polarized light, the result is a so-called diamagnetic line shape (Kahn *et al* 1969, Wittekoek *et al* 1975). In this case the energy difference $\Delta\hbar\omega$ occurs in the equation for ε_{xy} and the oscillator strengths of the two transitions for oppositely polarized light are taken to be equal. The magneto-optical transitions of type k will also contribute to the diagonal part of the dielectric tensor ε_{xx}, the contribution being of the form indicated in equation (5), with $f_k = \frac{1}{2}(f_k^- + f_k^+)$.

3. Experimental method

$Fe_{0.28}TaS_2$ was synthesized by heating together appropriate amounts of the elements at 850 °C for ten days. After repowdering the product was heated again for ten days. Single crystals were grown by iodine vapour transport in a temperature gradient from 950 to 800 °C for 15 days. The cell parameters were determined by means of X-ray powder diffraction to be $a = 5.763$ Å and $c = 12.227$ Å. The diffraction pattern showed a $\sqrt{3} \times \sqrt{3}$ superstructure indicating ordering of the iron ions between the sandwiches. The sample prepared in this way had a composition $Fe_{0.28}TaS_2$, as deduced from chemical analysis. The sample is ferromagnetic with a measured Curie temperature of 70 K and the magnetic moment of iron is directed perpendicular to the layers. The measured magnetic moment is $3.86\mu_B$ per Fe atom at 4.2 K (Dijkstra *et al* 1989). The crystals as grown from the vapour transport are platelets of area 15×20 mm^2 with a thickness of 0.1 mm and have nice shiny faces suitable for optical reflectivity measurements.

Ellipsometry measurements were carried out with the method and the equipment developed by Castelijns *et al* (1975), and later improved by Van der Heide *et al* (1984). The light source was a 150 W xenon lamp, and the monochromator had a resolution of 5 nm in the region 0.5 to 5.0 eV. Glan–Thomson prisms or Glan prisms were used as polarizers and analysers depending on the photon energy range. The reflected light passed through an analyser and the resulting intensity of the light for different analyser settings was measured with a photomultiplier or PbS cell depending on the photon energy range. The reproducibility of the polarizer and analyser settings is approximately 0.03°. At a given photon energy and for two polarizer settings at +45° and −45° with respect to the plane of incidence, the intensity after reflection was measured for eight analyser settings 45° apart. From the 16 measured intensities four sets of the ellipsometry parameters $\tan\psi$ and $\cos\Delta$ could be calculated. The (real) ellipsometry parameters Δ and ψ are defined in terms of the (complex) amplitude reflectivities r_s and r_p (for waves polarized perpendicular and parallel to the plane of incidence, respectively) by the relation $r_p/r_s = e^{\Delta}\tan\psi$. The experimental procedure just described eliminates at least some of the systematic errors, and makes it possible to estimate the statistical errors of the measurements (van der Heide *et al* 1984). Two different ellipsometry measurements of the reflection from a crystal face perpendicular to the c-axis were carried out at angles of incidence of 64° and 74° for each photon energy.

The errors in the ellipsometry results are larger than is usually the case for measurements on well polished crystals of good quality. The reason is that the reflecting surfaces of these layered materials are natural surfaces that cannot be polished. These natural surfaces are nice and shiny, and reflect light well, but for the thin crystals these surfaces are not very flat. This leads to variations of the angle of incidence, which can easily be a few degrees, and this is the main origin of the large errors in the data. The other errors in the ellipsometric measurements are much smaller (much less than 1°).

In addition we have also measured the reflection under near normal incidence in the photon energy range 1.5–5 eV with a simple set-up, using a photomultiplier.

The magneto-optical Kerr effect was measured in the polar configuration. We used a polarization modulation technique similar to that described by Sato (1981). A 600 W xenon lamp is used as a light source. The monochromatized light is chopped and polarized. The polarization state of the light is modulated with a frequency of 50 kHz by a photoelastic modulator. After reflection from the sample the light is detected by a photomultiplier (1.5–5 eV) or a Ge photodiode (0.75–1.5 eV). From the intensities of the DC signal and the AC signals with frequencies of 50 kHz and 100 kHz the Kerr rotation and ellipticity can be calculated (Sato 1981, Feil 1987).

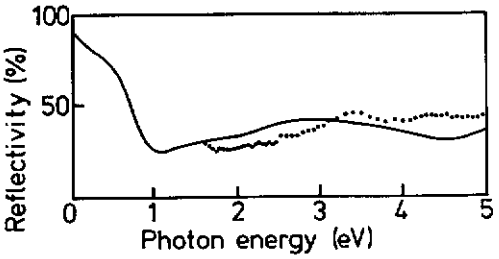

Figure 1. Reflectivity at 300 K for normal incidence of a single-crystal surface perpendicular to the *c*-axis of $Fe_{0.28}TaS_2$, dotted curve; $Fe_{0.33}TaS_2$, full curve (according to Parkin and Beal 1980).

The measurements were carried out in a cryostat. An unwanted effect of performing the measurements in the cryostat is the Faraday effect of the windows. Because of the very high coercivity the $Fe_{0.28}TaS_2$ single-crystal sample could not be saturated in a field of 5 T at 4.2 K. Therefore the measurements were carried out at 40 K and the sample was saturated in a field of 4 T. The remanence was about 85% of the saturation magnetization, which is high enough to allow measurements without an applied field, Thus eliminating the Faraday effect of the windows.

4. Experimental results

In figure 1 we show measurements at room temperature of the normal-incidence reflectivity of our sample $Fe_{0.28}TaS_2$ ($T_c = 70$ K) and data reported by Parkin and Beal (1980) for a sample $Fe_{0.33}TaS_2$ ($T_c = 40$ K). The difference between the two curves can at least in part be ascribed to the different compositions of the two samples.

The output of the ellipsometry experiments are the values of $\cos\Delta$ and $\tan^2\psi$ for two angles of incidence $\varphi = 64°$ and $\varphi = 74°$ as a function of photon energy in the region 0.6–5 eV. Values of ε_{xx} and ε_{zz} were obtained by a fitting procedure of calculated curves of $\tan^2\psi$ and $\frac{1}{2}(1 - \cos\Delta)$ as a function of angle of incidence φ to the values obtained by ellipsometry. The observed value of the normal incidence reflectivity ($\varphi = 0°$) was used as extra input in the fitting procedures. Some typical results are given in figure 2. The curves a and b clearly show that the values of $\tan^2\psi$ and $\cos\Delta$ depend strongly on the angle of incidence φ, especially near the Brewster angle.

We note that of the intensity reflectivities $R_s = |r_s|^2$ and $R_p = |r_p|^2$ the values of R_p at angles up to 50° and also the normal-incidence reflectivity are determined mainly by ε_{xx}. In the region $\varphi = 60$ to 80° R_p contains information about ε_{zz}. From the R_p and R_s curves at different energies it is seen that in the low-energy region (below 1 eV) the R_s curve is of the metallic type, whereas at higher energies the R_s curve is of the metallic type and the R_p curve is of the insulator type in the region $\varphi = 60$–80°. At the pseudoprinciple angle R_p is only a few percent. This anisotropy is most pronounced in $\cos\Delta$ at 2.2 eV, where $\cos\Delta = -1$ at $\varphi = 0°$ and $\cos\Delta$ is still -1 at $\varphi = 60°$, once more reflecting the dual character of the material: electrically well conducting in the layers and almost insulating in the direction normal to the layers (Parkin and Friend 1980b).

Figures 3 and 4 show the values of ε_{xx} and ε_{zz}, respectively, as functions of photon energy. The errors of about 0.1 in ε_{xx} and 0.05 in ε_{zz} (and somewhat larger errors in the infrared region near 1 eV) represent the spread in values deduced from measurements with different polarizer and analyser settings. The results for ε_{xx} have been analysed in terms of a Drude-type contribution for the intraband transitions and two Lorentz-type

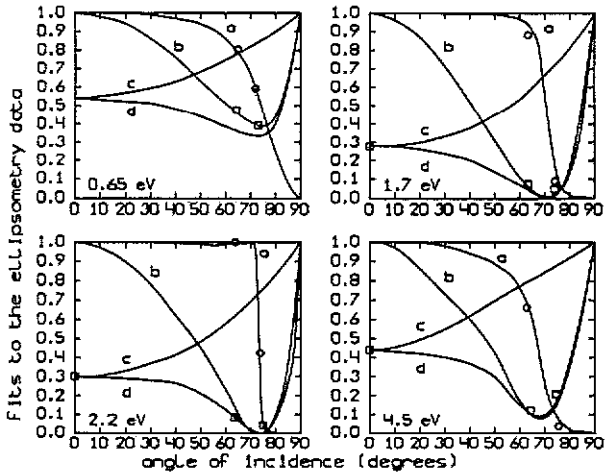

Figure 2. Fits for the determination of ε_{xx} and ε_{zz} from ellipsometry data taken at 300 K: squares at $\varphi = 0$; experimental values of normal-incidence reflectivity at 300 K; squares at $\varphi \approx 70°$, $\tan^2\psi$ from ellipsometry; circles at $\varphi \approx 70°$, $\frac{1}{2}(1 - \cos\Delta)$ from ellipsometry; full curves, fits to the experimental data. In addition: a, $(1 - \cos\Delta)/2$; b, $\tan^2\psi$; c, R_s; d, R_p. The size of the squares and circles is an estimation of the experimental errors. The photon energies are 0.65, 1.7, 2.2 and 4.5 eV.

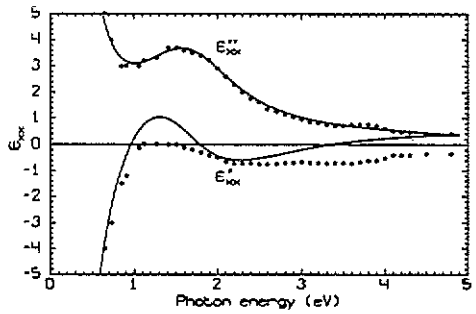

Figure 3. The diagonal part, $\varepsilon_{xx} = \varepsilon'_{xx} - i\varepsilon''_{xx}$, of the dielectric tensor at 300 K. The points show ε_{xx} from ellipsometry and reflectivity data. The full curves show ε_{xx} calculated for a Drude-type transition and two Lorentz-type contributions (parameters in table 1).

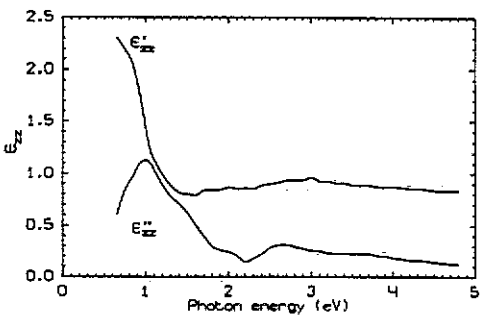

Figure 4. The diagonal part $\varepsilon_{zz} = \varepsilon'_{zz} - i\varepsilon''_{zz}$ of the dielectric tensor; obtained from ellipsometry measurements at 300 K.

contributions for the interband transitions, according to equation (3). The parameters are given in table 1. The calculated curve for ε''_{xx} as a function of photon energy shows a good fit to the experimental values (figure 3). The calculated values for ε'_{xx} are higher than the experimental values over the whole energy range. We find that ε_{xx} is of the metallic type and ε_{zz} is of the insulator type. In figures 5 and 6, respectively. the energy loss function and the function F (which is proportional to JDOS) are shown.

The Kerr rotation and ellipticity as a function of photon energy are given in figure 7. Rotations up to 0.6° and ellipticities up to 0.9° are found. A number of peaks are observed

Table 1. Parameters used to fit the diagonal part ε_{xx} at 300 K of the optical data. The values of f_k are calculated assuming a value of one electron per formula unit and the free-electron mass for m.

intraband:	$\hbar\omega_p = 2$ eV,	$\hbar\omega_s = 0.3$ eV	
interband:	$\hbar\omega_k$ (eV)	$\hbar\Gamma_k$ (eV)	f_k
	1.6	0.8	0.38
	3.8	1.9	0.17

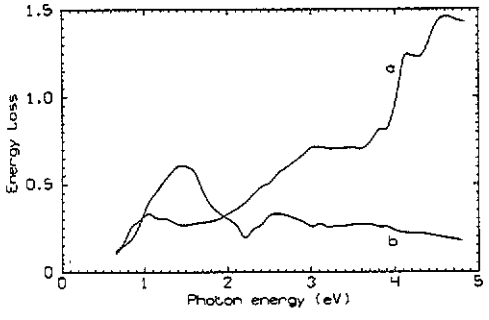

Figure 5. The energy loss function E_{loss} at 300 K. Curve a for an electric field normal to the c-axis, curve b for an electric field parallel to the c-axis.

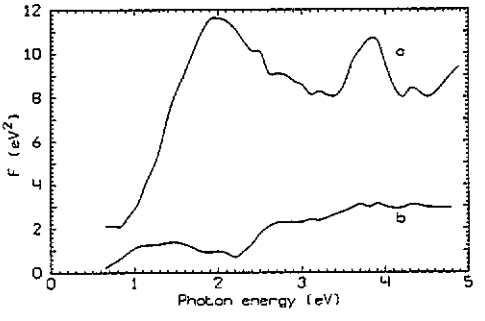

Figure 6. The function F at 300 K. Curve a for an electric field normal to the c-axis, curve b for an electric field parallel to the c-axis.

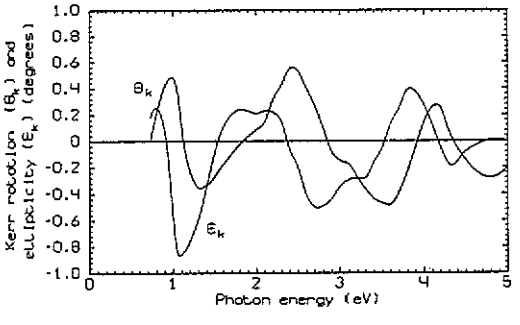

Figure 7. The Kerr rotation angle ϑ_K and Kerr ellipticity angle ε_K at 40 K.

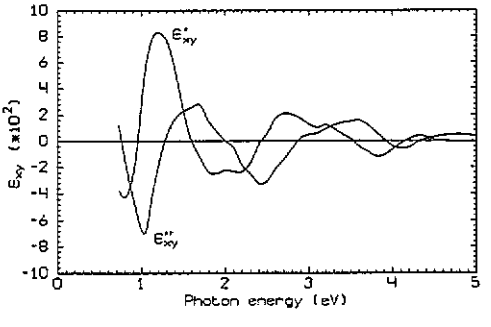

Figure 8. The off-diagonal elements $\varepsilon_{xy} = \varepsilon'_{xy} - i\varepsilon''_{xy}$ of the dielectric tensor at 40 K, as calculated from Kerr and ellipsometry data.

in the spectra. For the interpretation in terms of magneto-optical transitions we need to consider the off-diagonal element ε_{xy} of the dielectric tensor and not the peaks in the rotation and ellipticity. The off-diagonal element is calculated from the ellipsometry and Kerr data. The results are given in figure 8. We have made the assumption that ε_{xx} will not vary too much with temperature so that the room temperature ellipsometry measurements and low-temperature Kerr measurements can be combined to calculate ε_{xy}.

5. Discussion

From the experimental curves in figures 5 and 6 and the ε_{xx} and ε_{zz} data in figures 3 and 4 we can deduce information about the band structure. The two Lorentz-type transitions at 1.6 and 3.8 eV provide a reasonable fit for the contribution of interband transitions. The transition at 3.8 eV has a much larger width than the transition at 1.6 eV. These two interband transitions can also be seen in the function F (figure 6).

The dielectric constant in the low-frequency range describes the behaviour of the free carriers. The plasma energy $\hbar\omega_p = 2$ eV is related to the number of charge carriers and the effective mass. According to band structure calculations (Dijkstra *et al* 1989) the electrical conductivity is carried mainly by holes in the partly occupied Ta d_{z^2} band; the concentration of these holes is $N = 0.14$ holes per formula unit $Fe_{1/3}TaS_2$ as deduced from Hall measurements (Dijkstra *et al* 1989). Substituting this value of N, we deduce from the value of $\hbar\omega_p = 2$ eV a value of $m = 0.8m_0$ for the effective mass of the charge carriers (for the direction perpendicular to the c-axis). This is a reasonable value for the Ta d_{z^2} band, which is rather broad. From the values of N, m and ω_s we calculate for the DC electrical conductivity (for electrical fields perpendicular to the c-axis) $\sigma_{xx} = Ne^2/m\omega_s$ a value $\sigma_{xx} = 1.8 \times 10^5\ \Omega^{-1}\ m^{-1}$ at 300 K. This differs by a factor of 2.2 from the value $\sigma^0_{xx} = 4 \times 10^5\ \Omega^{-1}\ m^{-1}$ at 300 K, obtained directly from resistivity measurements (Dijkstra *et al* 1989). The difference between σ_{xx} and σ^0_{xx} can be explained by the energy dependence of the relaxation time $\tau = 1/\omega_s$.

The reflection spectrum of $Fe_{0.28}TaS_2$ for $E \perp c$ in the region above 1.5 eV is similar to that of the host compound 2H-TaS_2 (Parkin and Beal 1980). This indicates that the reflectivity in this region is dominated by transitions between energy bands derived mainly from Ta and S orbitals, with only minor contributions from Fe orbitals.

Looking at the curve for the energy loss function for an electric field parallel to the c-axis, we find a transition at 1.4 eV and probably weak transitions at 2.6 eV and 3.8 eV. The absence of strong interband transitions in ε_{zz} can be understood by considering the selection rules for Ta d–d transitions. Electric dipole transitions between d levels are not allowed in a free atom, but in a crystal of TaS_2 such transitions become possible because of strong hybridization of Ta 5d orbitals with orbitals of the ligand S atoms (Dijkstra *et al* 1989). Ta in 2H-TaS_2 and in $Fe_{0.28}TaS_2$ has a trigonally prismatic coordination of S atoms, which leads to a crystal-field splitting of the Ta 5d levels in the a′, e′ and e″ levels with m_l values of 0, ±2 and ±1, respectively (Huisman *et al* 1971) (m_l is the quantum number for the component of the orbital angular momentum along the c-axis). For an electric field perpendicular to the c-axis electric dipole transitions are only possible from the (partly) occupied a' level to the unoccupied e'' level. For an electric field parallel to the c-axis no electric dipole transitions between the Ta 5d levels are possible. Therefore all strong electric dipole transitions between Ta 5d bands are expected in ε_{xx} and not in ε_{zz}. Indeed the interband transition at 3.8 eV is quite pronounced in the JDOS. This transition is probably associated with transitions from Ta 5d (a′, the $5d_{z^2}$ band) to Ta 5d (e″) levels. The calculated band structure indeed shows unoccupied Ta 5d bands between 2 and 5 eV above the Ta $5d_{z^2}$ band with maxima in the density of states at 2 and 4 eV (Dijkstra *et al* 1989). These maxima correspond approximately to the energies of the Lorentz contributions at 1.6 eV and 3.8 eV. This analysis indicates that the observed transitions in ε_{xx} should be attributed mainly to transitions of electrons to the unoccupied Ta 5d bands.

The curves for the off-diagonal element ε_{xy} as a function of photon energy (figure 8) show several peaks. We have analysed these results in terms of Lorentz-like contributions as given in equation (5). It was possible to represent the experimental data

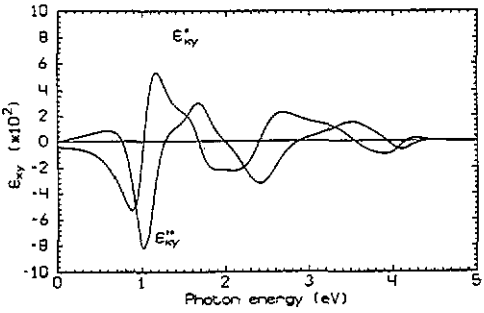

Figure 9. Calculated spectrum of ε_{xy}, obtained from five magneto-optical transitions with diamagnetic line shapes (equation (5)). The parameters for the contributions are given in table 2.

Table 2. Parameters used to fit the off-diagonal part ε_{xy} at 40 K of the optical data. The values of f_k are calculated assuming a value of one electron per formula unit and the free-electron mass for m.

$\hbar\omega_k$ (eV)	$\hbar\Gamma_k$ (eV)	$f_k\Delta\omega_k$ (10^{12} s^{-1})
1.02	0.25	−1.29
1.68	0.25	0.55
2.41	0.24	−3.87
3.51	0.50	2.42
4.09	0.28	−0.58

quite well with five transitions all with a diamagnetic line shape, at energies $\hbar\omega_k$ of 1.02, 1.68, 2.41, 3.51 and 4.09 eV (see figure 9). Only for the first transition is the fit not very good for ε'_{xy}. This indicates that this transition cannot be described by a diamagnetic line shape, but is actually of mixed character of paramagnetic and diamagnetic line shapes. The parameters of the fit to the experimental data are given in table 2. For a diamagnetic transition the assumption is made that the frequency difference between the transitions for left- and right-handed circularly polarized light is much smaller than the damping ($\Delta\omega \ll \Gamma$). The width of the magneto-optical transitions is not very large and the effective oscillator strength, $f\Delta(\hbar\omega)$, is quite small. We remark that the energies of these transitions do not correspond to the characteristic energies of the transitions used to describe ε_{xx}. This indicates that different optical transitions are responsible for the structures in ε_{xx} and ε_{xy}. Apparently the strong electric dipole transitions seen in ε_{xx} only have a small Kerr effect (small value of $f\Delta\omega$), and the magneto-optical transitions seen in ε_{xy} contribute little to ε_{xx} (small $f_- + f_+$).

For magneto-optical effects we need an exchange interaction and a spin–orbit coupling. For the Ta 5d levels a very large spin–orbit splitting is expected. According to the band structure calculation (Dijkstra *et al* 1989) the Ta d_{z^2} band in $Fe_{0.28}TaS_2$ is close to the Fermi level, the other Ta 5d bands lie at energies 2–5 eV above the Fermi level. The exchange splitting in the Ta 5d bands is quite small, so that we do not expect a large Kerr effect from Ta d–d transitions.

For the Fe 3d bands the spin–orbit splitting is much smaller, but the exchange splitting is quite large, about 3 eV (Dijkstra *et al* 1989). The Fe 3d spin-up bands lie completely below the Fermi level while the spin-down band lie almost completely above the Fermi level. Because of the small spin–orbit splitting for the Fe 3d bands, the energy difference

for transitions induced by left-hand and right-hand circularly polarized light will be small.

In transitions between the Fe 3d and Ta 5d states the combination of the large exchange splitting of the Fe 3d bands and the large spin–orbit coupling of the Ta 5d bands can lead to large magneto-optical effects. These transitions are not expected to have a large total oscillator strength $f_- + f_+$, and the contribution to ε_{xx} will be small. However, the contribution to ε_{xy} can be quite large.

The fact that we are dealing with diamagnetic transitions indicate that states with a small spin–orbit splitting are involved as initial (or final) states. As explained above these states must be the Fe 3d states. It seems unlikely that the final (or initial) state is also an Fe 3d state because the Fe d → d transitions are forbidden in first approximation and will be weak. We do not expect Fe 3d → Fe 3d intervalence charge transfer transitions to be important because of the large Fe–Fe interatomic distance. So the final (or initial) states have to be Ta 5d states or S 3p states. Because of the much larger density of states of Ta 5d than of S 3p in the energy region of interest the contribution of the Ta 5d states is expected to be larger than the contribution of the S 3p states. Therefore we ascribe the strong magneto-optical effects in $Fe_{0.28}TaS_2$ to transitions from Fe 3d to Ta 5d states.

In the band structure calculation reported for $Fe_{0.28}TaS_2$ spin–orbit interactions were not included. Therefore the calculated band structure cannot be used for a detailed interpretation of the strength of the magneto-optical effects.

6. Conclusions

The dielectric tensor of $Fe_{0.28}TaS_2$ was determined by means of ellipsometry and polar Kerr effect measurements. From the ellipsometry data it can be concluded that $Fe_{0.28}TaS_2$ has strongly anisotropic optical properties. For a polarization of the light with the electric field parallel to the layers, the optical properties are those of a metallic conductor. For a polarization perpendicular to the layers the optical properties are those of a semiconductor or insulator. This observation is in agreement with the anisotropy of the electrical conductivity.

The analysis of the ellipsometric data shows the presence of strong, broad optical absorption bands at about 1.6 and 3.8 eV in $Fe_{0.28}TaS_2$. These bands are attributed to transitions between Ta 5d energy bands. The contribution of these transitions to the magneto-optical properties is small.

The magneto-optical Kerr effect of $Fe_{0.28}Ta_2$ is quite large, and can be accounted for by five (diamagnetic) transitions between Fe 3d and Ta 5d states. The strong magneto-optical effects of these transitions are attributed to the combination of the large exchange splitting of the Fe 3d states and the large spin–orbit interaction of the Ta 5d states.

References

Azzam R M A and Bashara N M 1987 *Ellipsometry and Polarized Light* (Amsterdam: North-Holland)
Castelijns J H P, Derks J P C M and de Vroomen A R 1975 *J. Phys. F: Met. Phys.* 5 2407
Dijkstra J, Zijlema P J, van Bruggen C F, Haas C and de Groot R A 1989 *J. Phys.: Condens. Matter* 1 6363
Feil H 1987 *PhD Thesis* University of Groningen
Freiser M J 1968 *IEEE Trans. Magn.* **MAG-4** 152

van der Heide P A M, Baelde W, de Groot R A, de Vroomen A R and Mattocks P G 1984 *J. Phys. F: Met. Phys.* **14** 1745
Huisman R, de Jonge R, Haas C and Jellinek F 1971 *J. Solid State Chem.* **3** 56
Hummel R E 1971 *Optische Eigenschaften von Metallen und Legierungen* (Berlin: Springer) pp 16–42
Kahn F J, Pershan P S and Remeika J P 1969 *Phys. Rev.* **186** 891
Parkin S S P and Beal A R 1980 *Phil. Mag.* **42** 627
Parkin S S P and Friend R H 1980a *Phil. Mag.* **41** 65
—— 1980b *Phil. Mag.* **41** 95
Wittekoek S, Popma T J A, Robertson J M and Bongers P F 1975 *Phys. Rev.* B **12** 2777